

Robust Precoding via Characteristic Functions for VSAT to Multi-Satellite Uplink Transmission

Maik Röper^{*}, Bho Matthiesen^{*†}, Dirk Wübben^{*}, Petar Popovski^{‡,†}, and Armin Dekorsy^{*}

^{*} Gauss-Olbers Center, c/o University of Bremen, Dept. of Communications Engineering, 28359 Bremen, Germany

[†] University of Bremen, U Bremen Excellence Chair, Dept. of Communications Engineering, 28359 Bremen, Germany

[‡] Aalborg University, Department of Electronic Systems, 9220 Aalborg, Denmark

Email: {roeper, matthiesen, wuebben, dekorsy}@ant.uni-bremen.de, petarp@es.aau.dk

Abstract—The uplink from a very small aperture terminal (VSAT) towards multiple satellites is considered, in this paper. VSATs can be equipped with multiple antennas, allowing parallel transmission to multiple satellites. A low-complexity precoder based on imperfect positional information of the satellites is presented. The probability distribution of the position uncertainty and the statistics of the channel elements are related by the characteristic function of the position uncertainty. This knowledge is included in the precoder design to maximize the mean signal-to-leakage-and-noise ratio (SLNR) at the satellites. Furthermore, the performance w.r.t. the inter-satellite distance is numerically evaluated. It is shown that the proposed approach achieves the capacity for perfect position knowledge and sufficiently large inter-satellite distances. In case of imperfect position knowledge, the performance degradation of the robust precoder is relatively small.

Index Terms—LEO satellites, 3D networks, massive MIMO, beamforming, beamspace MIMO

I. INTRODUCTION

In future mobile networks, the terrestrial infrastructure will be extended by non-terrestrial networks (NTNs), consisting of unmanned aerial vehicles (UAVs), high altitude platform stations (HAPSSs) and communication satellites, forming a global heterogeneous 3D network. An integral component to these spatial networks are constellations of small satellites in low Earth orbits (LEOs) [1], [2]. This is because, in comparison to satellites in medium Earth orbit (MEO) and geostationary orbit (GEO), these constellations have reduced deployment costs and acceptable transmission delays [3], [4].

Recent results examine the application of multiple-input-multiple-output (MIMO) technologies to simultaneously communicate with multiple satellites [5]–[8]. In combination with formation flying techniques, which allow multiple satellites to move in clusters and act as a single entity [9]–[11], swarms of small satellites can form huge virtual antenna arrays with the promise of massive spectral efficiency improvements.

In [12], [13], optimal geometrical conditions for satellite swarms with respect to (w.r.t.) the channel capacity are derived. Additionally, a low-complexity linear transceiver design for the downlink from a satellite swarm towards a MIMO ground terminal has been proposed for the considered scenario. It has been observed that the derived transceiver achieves the channel capacity for sufficiently large inter-satellite distances and perfect position knowledge.

In case of imperfect position knowledge, the statistics of the uncertainty can be included to design a robust precoder. In [14] robust precoding under imperfect phase knowledge for multi-user downlink scenario is presented. The precoder is designed to achieve a given signal-to-interference-and-noise ratio (SINR) per user with minimum transmit power. In order to deal with the phase uncertainty, the SINR constraint is relaxed to be satisfied either only in mean, or with a given probabilistic. Similarly, in [15], [16] robust precoder with a relaxed average SINR constraint in the presence of phase uncertainties are presented. The precoder in [15] allows a trade-off between spectral and energy efficiency, while in [16] the energy efficiency for a hybrid precoder is maximized. A precoder under the strict constraint to ensure an SINR above a given threshold in case of bounded position uncertainty is given in [17]. There, different objective functions are numerically optimized, while the uncertainty region is sampled to obtain a finite set of constraints. In [18] another robust precoder for the multi-user downlink is presented to maximize the signal power of a user while keeping the interference leakage to other users within a bounded uncertainty region below a given threshold. A different approach to deal with position uncertainties is been presented in [13]. There, it is shown that the characteristic function (CF) of the position error is related to the autocorrelation matrix of the channel.

In this paper, we utilize the CF of the position uncertainty to present a novel robust precoder to maximize the mean signal-to-leakage-and-noise ratio (SLNR) [19] for very small aperture terminal (VSAT) to multi-satellite uplink applications. Therefore, different to [17], [18], our precoder is suitable for arbitrary probability distributions of the receiver positions. Furthermore, we obtain an analytic solution, and therefore the computational complexity is relatively low, as the precoder only requires an eigendecomposition. Furthermore, we show numerically that the proposed precoder achieves the capacity for sufficiently large inter-satellite distances and perfect position knowledge of the satellites at the VSAT.

The rest of the paper is organized as follows. Next, in Section II, the general system model and the performance benchmark for perfect channel state information (CSI) is presented. In Section III the proposed robust precoder is presented and numerically evaluated in Section IV. Finally, Section V concludes the paper.

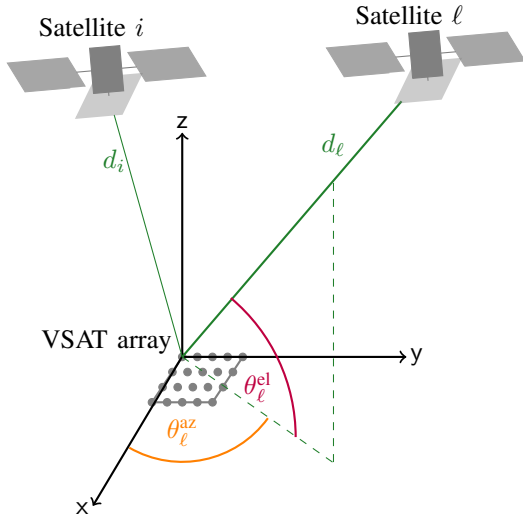


Fig. 1: Geometric relation between VSAT and satellite ℓ

II. SYSTEM MODEL AND PERFORMANCE BOUNDS

We consider the uplink from a single VSAT to a group of N_S single antenna satellites. The VSAT is equipped with a uniform rectangular array (URA) consisting of $N_T = N_T^x N_T^y \geq N_S$ antennas. Coordinates are stated in a VSAT-centric reference frame as depicted in Fig. 1. In particular, the z-axis points toward the VSAT's zenith, and the x- and y-axes are aligned with the VSAT's URA. Thus, N_T^x and N_T^y are the number of antennas of the VSAT in x- and y-direction, respectively. The position of satellite $\ell \in \{1, \dots, N_S\}$ is given by the triplet $(d_\ell, \theta_\ell^{\text{el}}, \theta_\ell^{\text{az}})$, where d_ℓ is the distance between satellite ℓ and the VSAT and $\theta_\ell^{\text{el}} \in [\theta_{\ell, \text{min}}^{\text{el}}, \pi/2]$ and $\theta_\ell^{\text{az}} \in [0, 2\pi)$ are the elevation and azimuth angles, respectively, as shown in Fig. 1.

The VSAT transmits N_S independent Gaussian data streams $\mathbf{s} \sim \mathcal{CN}(0, \mathbf{I}_{N_S})$, where \mathbf{I}_{N_S} is the identity matrix of dimension N_S . These streams are linearly precoded with $\mathbf{G} = [\mathbf{g}_1, \dots, \mathbf{g}_{N_S}] \in \mathbb{C}^{N_T \times N_S}$ to obtain the transmit signal $\mathbf{x} = \mathbf{G}\mathbf{s}$. The VSAT is subject to an average power constraint P_{Tx} , i.e.,

$$\mathbb{E}\{\mathbf{x}^H \mathbf{x}\} = \text{tr}\{\mathbf{G}\mathbf{G}^H\} \leq P_{\text{Tx}}. \quad (1)$$

The received signal y_ℓ at satellite ℓ is $y_\ell = \mathbf{h}_\ell^H \mathbf{x} + n_\ell$, where $\mathbf{h}_\ell \in \mathbb{C}^{N_T}$ is the channel from the VSAT to satellite ℓ and n_ℓ is circularly-symmetric complex white Gaussian noise with power σ_n^2 .

A. Channel and Error Model

We assume a line-of-sight (LOS) path between the VSAT and satellite ℓ and the received power from the non-LOS (NLOS) paths to be negligible small. Then, the elements of \mathbf{h}_ℓ differ only in their phase, but have the same magnitude [12], [20], [21]. Thus, we can define the channel vector \mathbf{h}_ℓ as a multiplication of a scalar factor $\alpha_\ell \in \mathbb{C}$ and a steering vector $\mathbf{a}_\ell \in \mathbb{C}^{N_T}$, whose elements have magnitude one, i.e.,

$$\mathbf{h}_\ell = \alpha_\ell \mathbf{a}_\ell. \quad (2)$$

The complex channel gain α_ℓ includes the signals attenuation and phase rotation due to the free space propagation and the atmospheric effects. The steering vector \mathbf{a}_ℓ depends on the satellite position. Due to the regular structure of the URA, it is helpful to separate \mathbf{a}_ℓ into two steering vectors $\mathbf{a}_\ell^x = [a_{\ell,1}^x, \dots, a_{\ell, N_T^x}^x]^T$ and $\mathbf{a}_\ell^y = [a_{\ell,1}^y, \dots, a_{\ell, N_T^y}^y]^T$, for the x- and y-direction, respectively, such that

$$\mathbf{a}_\ell = \mathbf{a}_\ell^x \otimes \mathbf{a}_\ell^y, \quad (3)$$

where \otimes denotes the Kronecker product. With the angles of departure (AoDs) as defined in Fig. 1 and given that the distance between the transmit antennas D_A at the VSAT is much smaller than the distance between the VSAT and satellite ℓ , i.e., $D_A \ll d_\ell$, the elements of the steering vectors are [22]

$$a_{\ell,m}^x = e^{-j\nu D_A (m-1) \cos(\theta_\ell^{\text{el}}) \cos(\theta_\ell^{\text{az}})}, \quad m = 1, \dots, N_T^x, \quad (4a)$$

$$a_{\ell,n}^y = e^{-j\nu D_A (n-1) \cos(\theta_\ell^{\text{el}}) \sin(\theta_\ell^{\text{az}})}, \quad n = 1, \dots, N_T^y, \quad (4b)$$

where ν is the wavenumber of the carrier wave. Furthermore, we define the space angles $\phi_\ell^x = \cos(\theta_\ell^{\text{el}}) \cos(\theta_\ell^{\text{az}})$ and $\phi_\ell^y = \cos(\theta_\ell^{\text{el}}) \sin(\theta_\ell^{\text{az}})$. While the AoDs θ_ℓ^{el} and θ_ℓ^{az} are related to the spherical coordinates, the space angles ϕ_ℓ^x and ϕ_ℓ^y are related to the Cartesian x- and y- coordinates of satellite ℓ , respectively. Note that in practical systems only imperfect knowledge of the satellites positions can be assumed. Let ξ_ℓ^x and ξ_ℓ^y be the estimation errors for the space angles in x- and y-direction, respectively, the estimated space angles are

$$\hat{\phi}_\ell^x = \phi_\ell^x + \xi_\ell^x, \quad \hat{\phi}_\ell^y = \phi_\ell^y + \xi_\ell^y. \quad (5)$$

Then, the $k = n + (m-1)N_T^y$ th element of the channel vector \mathbf{h}_ℓ can be written as

$$\begin{aligned} h_{\ell,k} &= \alpha_\ell a_{\ell,m}^x a_{\ell,n}^y \\ &= \alpha_\ell e^{-j\nu D_A ((m-1)(\hat{\phi}_\ell^x - \xi_\ell^x) + (n-1)(\hat{\phi}_\ell^y - \xi_\ell^y))}, \end{aligned} \quad (6)$$

which includes three statistically independent random variables from the transmitters perspective, i.e., α_ℓ , ξ_ℓ^x and ξ_ℓ^y . The complex channel gain α_ℓ is a circularly-symmetric random variable with variance $\mathbb{E}\{|\alpha_\ell|^2\} = \sigma_{\alpha_\ell}^2$. Note that the variance $\sigma_{\alpha_\ell}^2$ can be different for each satellite ℓ , due to the different path losses. For the estimation errors of the space angles ξ_ℓ^x and ξ_ℓ^y , we assume the same probability distribution for every satellite ℓ and for both directions. Their probability distribution is described by the characteristic function $\varphi_\xi(t)$ [23].

B. Upper bound on the channel capacity

To obtain an upper bound on the throughput performance, perfect CSI at the transmitter and receiver as well as instantaneous and error-free inter-satellite communication is assumed. Hence, perfect coordination between satellites is possible and the system can be modelled as an $N_T \times N_S$ MIMO system. The joint receive signal of all satellites is $\mathbf{y} = \mathbf{H}\mathbf{x} + \mathbf{n}$, with the channel matrix $\mathbf{H} = [\mathbf{h}_1, \dots, \mathbf{h}_{N_S}]^H$ and the noise vector $\mathbf{n} = [n_1, \dots, n_{N_S}]^T$, where the components of \mathbf{n} are

mutually independent. Let λ_μ be the μ th eigenvalue of $\mathbf{H}\mathbf{H}^H$, the capacity of this channel is [24]

$$C = \sum_{\mu=1}^{N_S} \log_2 \left(1 + \lambda_\mu \frac{p_\mu}{\sigma_n^2} \right), \quad (7)$$

where and p_μ is the optimal power allocated to the μ th stream. Given the power constraint $\sum_{\mu} p_\mu = P_{\text{Tx}}$, the optimal power allocation is obtained from the water-filling algorithm [24].

III. PROPOSED UPLINK APPROACH

In this section, we present a novel low-complexity robust precoder for uplink transmission from a VSAT to multiple satellites based on imperfect knowledge of the satellites positions. For sufficiently large distances between the satellites, the channel vectors become nearly orthogonal, i.e., $\mathbf{a}_i^H \mathbf{a}_\ell \approx 0$. In this case, the channel capacity is maximized, because the eigenvalues of $\mathbf{H}\mathbf{H}^H$ are almost equal [12]. Given orthogonal channels, the capacity can be achieved by transmitting independent data streams [24].¹ Thus, we assign one stream per satellite and then design the precoders. Given independent data streams, no inter-satellite communication is required for estimation and decoding because satellite ℓ can estimate and decode the transmitted symbol s_ℓ independently from the other satellites. Numerical results in Section IV-A show that this approach is, despite its simplicity, capacity achieving for sufficiently large orbital separations and perfect position knowledge of the satellites. The received signal at satellite ℓ is $y_\ell = \mathbf{h}_\ell^H \mathbf{g}_\ell s_\ell + \sum_{i \neq \ell} \mathbf{h}_\ell^H \mathbf{g}_i s_i + n_\ell$. Correspondingly, the instantaneous SINR Γ_ℓ at satellite ℓ is given as

$$\Gamma_\ell = \frac{|\mathbf{h}_\ell^H \mathbf{g}_\ell|^2}{\sum_{i \neq \ell} |\mathbf{h}_\ell^H \mathbf{g}_i|^2 + \sigma_n^2} \quad (8)$$

and the achievable rate R is equal to the sum rate

$$R = \sum_{\ell=1}^{N_S} \log_2 (1 + \Gamma_\ell). \quad (9)$$

The goal is to obtain precoders that maximize this rate. However, the exact values of \mathbf{h}_ℓ are not known but only their estimates based on $\hat{\phi}_\ell^x$ and $\hat{\phi}_\ell^y$. Furthermore, directly maximizing this sum rate is NP-hard and has, to the best of our knowledge, no easy analytical solution. In the following, we solve a slightly simplified version of this problem that, as will be seen later in Sec. IV, will result in a solution that is often close to the optimal throughput performance.

A. Problem Formulation

Observe that the SINRs Γ_ℓ in (8) are coupled through their denominator. Substituting Γ_ℓ in (9) with the instantaneous SLNR for satellite ℓ defined as

$$\gamma_\ell = \frac{|\mathbf{h}_\ell^H \mathbf{g}_\ell|^2}{\sum_{i \neq \ell} |\mathbf{h}_i^H \mathbf{g}_\ell|^2 + \sigma_n^2} \quad (10)$$

¹Observe that this does not imply the transmission of several independent messages. See, e.g., [25] or [26, Sec. 5.8.1].

and assuming equal power allocation among streams, leads to the substitute optimization problem

$$\max_{\mathbf{g}_\ell} \frac{|\mathbf{h}_\ell^H \mathbf{g}_\ell|^2}{\sum_{i \neq \ell} |\mathbf{h}_i^H \mathbf{g}_\ell|^2 + \sigma_n^2} \quad \text{s.t.} \quad \mathbf{g}_\ell^H \mathbf{g}_\ell \leq \frac{P_{\text{Tx}}}{N_S}, \quad (11)$$

which has to be solved for each $\ell \in \{1, \dots, N_S\}$. However, this problem still relies on the exact knowledge of the channels. Our goal is to design robust precoders that take the statistics of the estimation error into account. This can be achieved by optimizing over the mean SLNR $\bar{\gamma} = \mathbb{E}\{\gamma\}$, i.e.,

$$\max_{\mathbf{g}_\ell} \mathbb{E} \left\{ \frac{|\mathbf{h}_\ell^H \mathbf{g}_\ell|^2}{\sum_{i \neq \ell} |\mathbf{h}_i^H \mathbf{g}_\ell|^2 + \sigma_n^2} \right\} \quad \text{s.t.} \quad \mathbf{g}_\ell^H \mathbf{g}_\ell \leq \frac{P_{\text{Tx}}}{N_S}, \quad (12)$$

where the expectation is taken w.r.t. the channel vectors $\mathbf{h}_1, \dots, \mathbf{h}_{N_S}$. Then, the robust precoders $\mathbf{g}_\ell^{\text{rob}}$ are a solution of (12).

B. Robust Precoding via CF

The solution of (12) requires a closed-form expression of the autocorrelation matrix of the channel $\mathbb{E}\{\mathbf{h}_\ell \mathbf{h}_\ell^H\}$, which is closely related to the autocorrelation matrix of the steering vectors. In particular, let $\mathbf{R}_{\mathbf{a}_\ell} = \mathbb{E}\{\mathbf{a}_\ell \mathbf{a}_\ell^H\}$ be the autocorrelation matrix of the steering vector \mathbf{a}_ℓ . With (3) and due to the statistical independence of the position uncertainties ξ_ℓ^x and ξ_ℓ^y , we can write

$$\mathbf{R}_{\mathbf{a}_\ell} = \mathbb{E}\{\mathbf{a}_\ell \mathbf{a}_\ell^H\} = \mathbb{E}\left\{(\mathbf{a}_\ell^x \otimes \mathbf{a}_\ell^y)(\mathbf{a}_\ell^x \otimes \mathbf{a}_\ell^y)^H\right\} \quad (13a)$$

$$= \mathbb{E}\{\mathbf{a}_\ell^x \mathbf{a}_\ell^{xH}\} \otimes \mathbb{E}\{\mathbf{a}_\ell^y \mathbf{a}_\ell^{yH}\} = \mathbf{R}_{\mathbf{a}_\ell^x} \otimes \mathbf{R}_{\mathbf{a}_\ell^y}. \quad (13b)$$

The random variables in $\mathbf{R}_{\mathbf{a}_\ell^x}$ and $\mathbf{R}_{\mathbf{a}_\ell^y}$ are only the estimation errors ξ_ℓ^x and ξ_ℓ^y , respectively. The characteristic function $\varphi_\xi(t)$ of these random variables is defined as [23]

$$\varphi_\xi(t) = \mathbb{E}\left\{e^{jt\xi_\ell^x}\right\} = \mathbb{E}\left\{e^{jt\xi_\ell^y}\right\}. \quad (14)$$

Thus, the (m, m') th element of the autocorrelation matrix $\mathbf{R}_{\mathbf{a}_\ell^x}$ is given by

$$[\mathbf{R}_{\mathbf{a}_\ell^x}]_{m, m'} = \mathbb{E}\left\{e^{-j\nu D_A(m-m')(\hat{\phi}_\ell^x - \xi_\ell^x)}\right\} \quad (15a)$$

$$= e^{-j\nu D_A(m-m')\hat{\phi}_\ell^x} \varphi_{\xi_\ell^x}(\nu D_A(m' - m)). \quad (15b)$$

The elements of $\mathbf{R}_{\mathbf{a}_\ell^y}$ are given, analogously.

Now, we can formulate the optimal precoder, as stated in the following theorem.

Theorem 1. *The robust precoder, i.e., the solution to (12), is*

$$\mathbf{g}_\ell^{\text{rob}} = \frac{P_{\text{Tx}}}{N_S} \boldsymbol{\psi}_{\ell, \max}, \quad (16)$$

where $\boldsymbol{\psi}_{\ell, \max}$ is the eigenvector corresponding to the largest eigenvalue of $(\sum_{i \neq \ell} \sigma_{\alpha_i}^2 \mathbf{R}_{\mathbf{a}_i} + N_S \sigma_n^2 / P_{\text{Tx}} \mathbf{I}_{N_T})^{-1} \sigma_{\alpha_\ell}^2 \mathbf{R}_{\mathbf{a}_\ell}$.

Proof: Note that α_ℓ , ξ_ℓ^x and ξ_ℓ^y are statistically independent of α_i , ξ_i^x and ξ_i^y for $i \neq \ell$. Therefore, \mathbf{h}_ℓ and \mathbf{h}_i are statistically independent, too. Thus, we can rewrite the objective function (12) as

$$\bar{\gamma}_\ell = \mathbb{E} \left\{ \frac{|\mathbf{h}_\ell^H \mathbf{g}_\ell|^2}{\sum_{i \neq \ell} |\mathbf{h}_i^H \mathbf{g}_\ell|^2 + \sigma_n^2} \right\} \quad (17a)$$

$$= \frac{\mathbf{g}_\ell^H \mathbb{E} \{ \mathbf{h}_\ell \mathbf{h}_\ell^H \} \mathbf{g}_\ell}{\mathbf{g}_\ell^H \left(\sum_{i \neq \ell} \mathbb{E} \{ \mathbf{h}_i \mathbf{h}_i^H \} + \frac{\sigma_n^2}{p_\ell} \mathbf{I}_{N_T} \right) \mathbf{g}_\ell} \quad (17b)$$

where $p_\ell = \mathbf{g}_\ell^H \mathbf{g}_\ell$ is the transmit power of the ℓ th stream.

With (2) and (13), the expected value in (17b) can be written as $\mathbb{E} \{ \mathbf{h}_\ell \mathbf{h}_\ell^H \} = \sigma_{\alpha_\ell}^2 \mathbf{R}_{\mathbf{a}_\ell}$. Furthermore, the term in (17b) is monotonically increasing with the transmit power p_ℓ . Therefore, at the optimum solution the constraint must be active, i.e., $p_\ell = P_{\text{Tx}}/N_S$. Correspondingly, the optimization problem (12) is equivalent to

$$\max_{\mathbf{g}_\ell} \frac{\sigma_{\alpha_\ell}^2 \mathbf{g}_\ell^H \mathbf{R}_{\mathbf{a}_\ell} \mathbf{g}_\ell}{\mathbf{g}_\ell^H \left(\sum_{i \neq \ell} \sigma_{\alpha_i}^2 \mathbf{R}_{\mathbf{a}_i} + \frac{N_S \sigma_n^2}{P_{\text{Tx}}} \mathbf{I} \right) \mathbf{g}_\ell} \quad (18a)$$

$$\text{s.t. } \mathbf{g}_\ell^H \mathbf{g}_\ell = \frac{P_{\text{Tx}}}{N_S} \quad (18b)$$

The objective function (18a) is a generalized Rayleigh quotient. Consequently, the maximum is achieved by the scaled eigenvector corresponding to the largest eigenvalue of $\left(\sum_{i \neq \ell} \sigma_{\alpha_i}^2 \mathbf{R}_{\mathbf{a}_i} + N_S \sigma_n^2 / P_{\text{Tx}} \mathbf{I}_{N_T} \right)^{-1} \mathbf{R}_{\mathbf{a}_\ell}$ [19], i.e., the precoder $\mathbf{g}_\ell^{\text{rob}}$ must be proportional to $\boldsymbol{\psi}_{\ell, \text{max}}$. Given the constraint (18b), the only solution is given by (16). ■

The precoder in Theorem 1 optimizes (12) for any probability distribution of ξ_ℓ^x and ξ_ℓ^y . For the special case of perfect position knowledge, we obtain a closed-form solution, as stated in the following corollary.

Corollary 1. *For perfect knowledge of the steering vectors, the optimal precoder for (12) is*

$$\mathbf{g}_\ell^{\text{per}} = \beta \left(\sum_{i=1}^{N_S} \sigma_{\alpha_i}^2 \mathbf{a}_i \mathbf{a}_i^H + \frac{N_S \sigma_n^2}{P_{\text{Tx}}} \mathbf{I}_{N_T} \right)^{-1} \mathbf{a}_\ell \quad (19)$$

where the normalization coefficient β is chosen such that $\text{tr} \{ \mathbf{G}_\ell \mathbf{G}_\ell^H \} = P_{\text{Tx}}/N_S$.

Proof: For perfect position knowledge, i.e., $\xi_\ell^x = \xi_\ell^y = 0$, the characteristic function $\varphi_\xi(t)$ becomes one. Thus, the objective function is

$$\bar{\gamma} |_{\varphi_\xi(t)=1} = \frac{\sigma_{\alpha_\ell}^2 \mathbf{g}_\ell^H \mathbf{a}_\ell \mathbf{a}_\ell^H \mathbf{g}_\ell}{\mathbf{g}_\ell^H \left(\sum_{i \neq \ell} \sigma_{\alpha_i}^2 \mathbf{a}_i \mathbf{a}_i^H + \frac{N_S \sigma_n^2}{P_{\text{Tx}}} \mathbf{I} \right) \mathbf{g}_\ell}. \quad (20)$$

Consequently, the optimal precoder with perfect position knowledge must be a scaled eigenvector of $\left(\sum_{i \neq \ell} \sigma_{\alpha_i}^2 \mathbf{a}_i \mathbf{a}_i^H + N_S \sigma_n^2 / P_{\text{Tx}} \mathbf{I}_{N_T} \right)^{-1} \mathbf{a}_\ell \mathbf{a}_\ell^H$. Such an eigenvector is given by (19) [27]. ■

Furthermore, given perfect position knowledge and orthogonal channels, the following corollary holds as well.

Corollary 2. *If $\forall i \neq \ell$, the steering vectors \mathbf{a}_i and \mathbf{a}_ℓ are orthogonal and the path losses $|\alpha_i|^2$ and $|\alpha_\ell|^2$ are the same, i.e., $\mathbf{a}_i^H \mathbf{a}_\ell = 0$ and $|\alpha_i|^2 = |\alpha_\ell|^2$, respectively, the precoder with perfect position knowledge (19) is capacity achieving.*

Proof: Note that the precoder (19) is capacity achieving, if its columns are given by the right singular vectors of \mathbf{H}

and the norm of each column is equal to the optimal power allocation, obtained via the water-filling algorithm [24]. Let $\mathbf{A} = [\mathbf{a}_1, \dots, \mathbf{a}_{N_S}]$, with $\mathbf{A}^H \mathbf{A} = N_T \mathbf{I}_{N_S}$, and $|\alpha_i|^2 = |\alpha_\ell|^2 = |\alpha|^2$, for all i and ℓ , the precoder matrix $\mathbf{G}^{\text{per}} = [\mathbf{g}_1^{\text{per}}, \dots, \mathbf{g}_{N_S}^{\text{per}}]$ can be written as

$$\mathbf{G}^{\text{per}} = \beta \left(|\alpha|^2 \mathbf{A} \mathbf{A}^H + \frac{N_S \sigma_n^2}{P_{\text{Tx}}} \mathbf{I}_{N_T} \right)^{-1} \mathbf{A} \quad (21a)$$

$$= \beta \mathbf{A} \left(|\alpha|^2 \mathbf{A}^H \mathbf{A} + \frac{N_S \sigma_n^2}{P_{\text{Tx}}} \mathbf{I}_{N_S} \right)^{-1} \quad (21b)$$

$$= \sqrt{P_{\text{Tx}}/N_T} \mathbf{A}, \quad (21c)$$

where (21b) follows from the the matrix inversion lemma [28] and (21c) is obtained due to the orthogonal steering vectors.

Now, given the channel model (2), the matrix \mathbf{H} can be factorized via the singular value decomposition (SVD) as

$$\mathbf{H} = (\text{diag}(\alpha_1, \dots, \alpha_{N_S}) \mathbf{A})^H = \mathbf{U} \boldsymbol{\Sigma} \mathbf{V}^H, \quad (22)$$

where $\mathbf{U} = 1/|\alpha| \text{diag}(\alpha_1, \dots, \alpha_{N_S})^H$ and $\mathbf{V} = 1/\sqrt{N_T} [\mathbf{A}, \mathbf{v}_{N_S+1}, \dots, \mathbf{v}_{N_T}]$ are unitary matrices. The vectors $\{\mathbf{v}_{N_S+1}, \dots, \mathbf{v}_{N_T}\}$ are the right singular vectors belonging to the nullspace of the channel matrix \mathbf{H} . Furthermore, $\boldsymbol{\Sigma} = [|\alpha| \sqrt{N_T} \mathbf{I}_{N_S}, \mathbf{0}_{N_S \times (N_T - N_S)}]$, where $\mathbf{0}_{N_S \times (N_T - N_S)}$ is an all zero matrix of dimension $N_S \times (N_T - N_S)$, is a rectangular diagonal matrix with the singular values of \mathbf{H} on its diagonal. Thus, the precoder matrix (21c) is proportional to the right singular vectors of \mathbf{H} , which do not belong to the nullspace. Finally, as there is only a single non-zero singular value with multiplicity N_S , the capacity is achieved by allocating the same power to each right singular vector. This is given by the precoder \mathbf{G}^{per} , which concludes the proof. ■

Note that in Corollary 2, the assumptions on the channel are very strict. In the next section, we show numerically that the precoder also achieves the capacity in more general cases.

IV. NUMERICAL EVALUATIONS

To evaluate the proposed precoder approach, we consider a satellite swarm in triangle formation with a fixed inter-satellite distance D_S between any of these $N_S = 3$ satellites. The VSAT is equipped with a 32×32 URA with an antenna spacing of $D_A = 2.5$ cm. The antenna gain at the VSAT and the satellites are $\zeta_{\text{Tx,dB}} = 43.2$ dBi $- 10 \log_{10}(N_T) \approx 13.1$ dBi and $\zeta_{\text{Rx,dB}} = 30.5$ dBi $- 10 \log_{10}(N_S) \approx 25.7$ dBi, respectively, to match the 3GPP recommendation [29]. The carrier frequency and the noise power are $f_c = 30$ GHz and $P_N = -120$ dBW, respectively. The channel is modeled as a pure LOS channel. Thus, the scaling factor is $\alpha_\ell = 1/L_\ell e^{j\phi_{\ell,0}}$, where $\phi_{\ell,0} \sim \mathcal{U}(0, 2\pi)$ is a random phase rotation and L_ℓ is the path loss, including the antenna gains $\zeta_{\text{Tx,dB}}$ and $\zeta_{\text{Rx,dB}}$, free space path loss, shadow fading, clutter loss [30], atmospheric gas absorption [31] and tropospheric scintillation [32], [33]. Furthermore, the altitude of the satellites is $d_0 = 600$ km and the minimum elevation angle is $\theta_{\ell, \text{min}}^{\text{el}} = 30^\circ$.

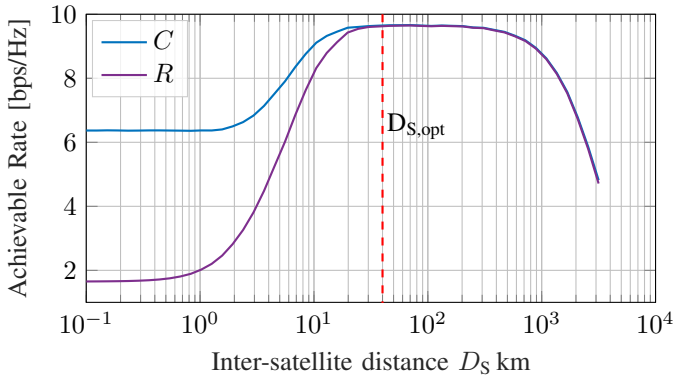


Fig. 2: Achievable rate for different inter-satellite distances D_S and perfect position knowledge

A. Optimal Inter-Satellite Distance

In [12], the optimal inter-satellite distance for a simplified downlink scenario has been derived. In this subsection, we evaluate the performance w. r. t. the inter-satellite distance for an uplink scenario and a fixed transmit power of $P_{Tx} = 5$ dBW. Given the altitude $d_0 = 600$ km, the minimum elevation angle $\theta_{\ell, \min}^{\text{el}} = 30^\circ$, $N_T^x = 32$ antennas along the x-axis and $\nu D_A = 5\pi$, the analytic solution for the optimum inter-satellite distance is $D_{S, \text{opt}} \approx 40$ km [12]. In Fig. 2, the channel capacity C and the sum rate R with the proposed precoder and perfect position knowledge are shown. It can be observed that both rates increase with increasing inter-satellite distances D_S up to a certain distance and then slightly decrease. The inter-satellite distance, where both rates achieve their maximum matches with the analytic solution $D_{S, \text{opt}}$ from [12]. For $D_S < D_{S, \text{opt}}$, the sum rate is significantly smaller than the channel capacity, due to the relatively big difference between the maximum and minimum eigenvalue. If $D_S \geq D_{S, \text{opt}}$, all eigenvalues are approximately the same because $\mathbf{a}_i^H \mathbf{a}_\ell \approx 0$, for $i \neq \ell$. Therefore, the difference between the sum rate and the capacity is negligible small. The performance degradation for very large inter-satellite distances is due to the increased path loss averaged over the satellites.

B. Robust Precoding

Now, we evaluate the performance of the proposed robust precoder (16) for a constant inter-satellite distance $D_S = 40$ km. Furthermore, we assume two different error distributions of the position uncertainty. The robust precoder requires knowledge about the CF of the probability distribution. Therefore, the CFs of both probability distribution are given in the appendix. For comparison, a heuristic precoder $\mathbf{g}_\ell^{\text{heu}}$ for imperfect knowledge is obtained by substituting the true steering vectors by the estimated ones in (19), i.e.,

$$\mathbf{g}_\ell^{\text{heu}} = \beta \left(\sum_{i \neq \ell} \sigma_{\alpha_i}^2 \hat{\mathbf{a}}_i \hat{\mathbf{a}}_i^H + \frac{N_S \sigma_n^2}{P_{Tx}} \mathbf{I}_{N_T} \right)^{-1} \hat{\mathbf{a}}_\ell. \quad (23)$$

Note that for perfect position knowledge, the heuristic precoder (23) as well as the robust precoder (16) are the same.

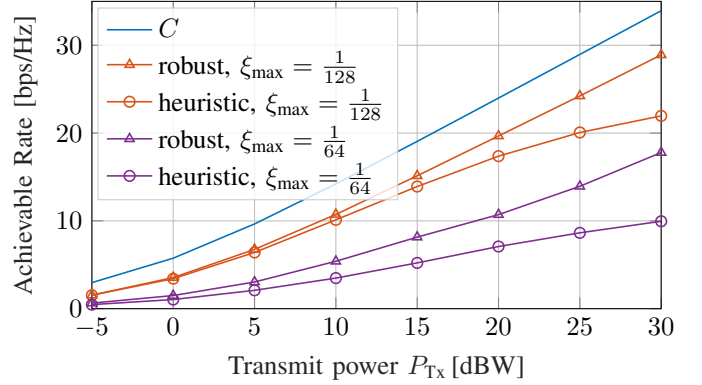


Fig. 3: Achievable rate of robust and heuristic precoder in case of uniformly distributed position uncertainty

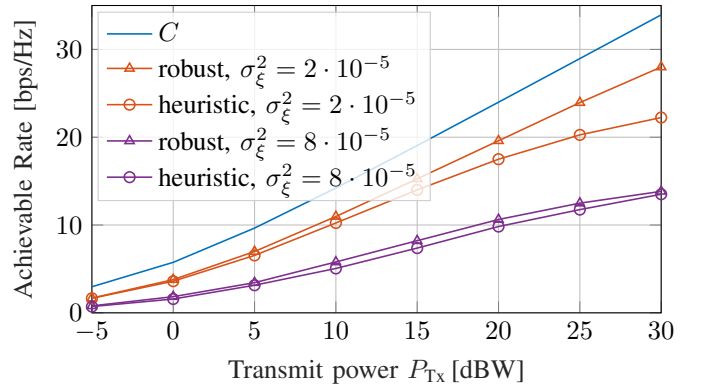


Fig. 4: Achievable rate of robust and heuristic precoder in case of gaussian distributed position uncertainty

In Fig. 3, the achievable rates for the proposed robust and heuristic precoder (16) and (23), respectively, are shown for a uniformly distributed position uncertainty. Thus, the error of the space angles are uniformly distributed, i.e., $\xi_\ell^x, \xi_\ell^y \sim \mathcal{U}(-\xi_{\max}, \xi_{\max})$. It can be seen, that the sum rate with the heuristic precoder degrades, especially for high transmit powers. For the robust precoder, the sum rate is almost parallel to the channel capacity. Thus, the performance degradation is less severe and the robust precoder clearly outperforms the heuristic precoder.

In Fig. 4, the corresponding performance for Gaussian distribution, i.e., $\xi_\ell^x, \xi_\ell^y \sim \mathcal{N}(0, \sigma_\xi^2)$, is shown. The variance σ_ξ^2 is chosen such that it is almost the same as for the uniformly distributed error in Fig. 3. It can be seen that the performance gain of the robust precoder compared to the heuristic precoder is smaller than for uniformly distributed position uncertainty. On the one hand, the slope for the robust precoder is not parallel to the channel capacity anymore. Instead, the sum rate degrades stronger for high transmit powers. On the other hand, the impact of gaussian distributed position uncertainty seem to be less severe for the heuristic precoder.

V. CONCLUSION

In this paper, a novel robust precoder for LOS communication is presented. Instead of full CSI, the proposed precoder

is based on the second order statistics of the channel, which include imperfect position knowledge of the receivers, as well as statistical knowledge of the position uncertainty and the long term fading of the channel. The position uncertainty of the receivers induce a correlated phase error among the transmit antennas. It has been shown that the resulting statistic of the phase error and the channel statistics are connected via the CF of the phase error distribution. Furthermore, the proposed approach to transmit data from a VSAT to multiple satellite has low complexity and is capacity achieving for perfect position knowledge of the satellites and sufficiently large distances between them.

ACKNOWLEDGMENT

This research was supported in part by the German Federal Ministry of Education and Research (BMBF) within the project Open6GHub under grant number 16KISK016A, the German Research Foundation (DFG) under Germany's Excellence Strategy (EXC 2077 at University of Bremen, University Allowance) and by the European Space Agency (ESA) within the SatNEx V activity WI Y2.2-A.

APPENDIX A

CHARACTERISTIC FUNCTION

a) *Uniform Distribution:* Let $\xi_{\text{uni}} \sim \mathcal{U}(-v_{\text{max}}, v_{\text{max}})$ be uniformly distributed in the interval $[-\xi_{\text{max}}, \xi_{\text{max}}]$. Then, the characteristic function φ_{U} is a sinc-function, i.e.,

$$\varphi_{\text{U}}(t) = \int_{-\xi_{\text{max}}}^{\xi_{\text{max}}} \frac{1}{2\xi_{\text{max}}} e^{j\xi t} d\xi \quad (24a)$$

$$= \frac{\sin(t\xi_{\text{max}})}{t\xi_{\text{max}}} = \text{sinc}(t\xi_{\text{max}}). \quad (24b)$$

b) *Gaussian Distribution:* Let $\xi_{\text{gau}} \sim \mathcal{N}(0, \sigma_{\xi}^2)$ be gaussian distributed. Then the characteristic function φ_{G} follows also a gaussian function [23, Example 8.5], i.e.,

$$\varphi_{\text{G}}(t) = \int_{-\infty}^{\infty} \frac{1}{\sigma_{\xi}\sqrt{2\pi}} e^{-\left(\frac{\xi}{\sigma_{\xi}}\right)^2} e^{j\xi t} d\xi = e^{-\frac{t^2\sigma_{\xi}^2}{2}}. \quad (25)$$

REFERENCES

- [1] O. Kodheli *et al.*, "Satellite communications in the new space era: A survey and future challenges," *IEEE Communications Surveys Tutorials*, vol. 23, no. 1, pp. 70–109, Jan.–Mar. 2021.
- [2] 3GPP TR 38.863, "Technical Specification Group Radio Access Network; Solutions for NR to support non-terrestrial networks (NTN): Non-terrestrial networks (NTN) related RF and co-existence aspects (Release 17)," Sep. 2022.
- [3] B. Di, L. Song, Y. Li, and H. V. Poor, "Ultra-dense LEO: Integration of satellite access networks into 5G and beyond," *IEEE Trans. Wireless Commun.*, vol. 26, no. 2, pp. 62–69, Apr. 2019.
- [4] I. Leyva-Mayorga, B. Soret, M. Röper, D. Wübben, B. Matthiesen, A. Dekorsy, and P. Popovski, "LEO small-satellite constellations for 5G and beyond-5G communications," *IEEE Access*, vol. 8, Oct. 2020.
- [5] P.-D. Arapoglou, K. Liolis, M. Bertinelli, A. Panagopoulos, P. Cottis, and R. De Gaudenzi, "Mimo over satellite: A review," *IEEE Commun. Surveys Tuts.*, vol. 13, no. 1, pp. 27–51, 1st Quart. 2011.
- [6] D. Goto, H. Shibayama, F. Yamashita, and T. Yamazato, "LEO-MIMO satellite systems for high capacity transmission," in *Proc. IEEE Glob. Commun. Conf. (GLOBECOM)*, Abu Dhabi, United Arab Emirates, Dec. 2018.
- [7] C. Hofmann, K.-U. Storek, R. T. Schwarz, and A. Knopp, "Spatial mimo over satellite: A proof of concept," in *Proc. IEEE Int. Conf. Commun. (ICC)*, May 2016.
- [8] R. Richter, I. Bergel, Y. Noam, and E. Zehavi, "Downlink cooperative MIMO in LEO satellites," *IEEE Access*, vol. 8, Nov. 2020.
- [9] C. Verhoeven, M. Bentum, G. Monna, J. Rotteveel, and J. Guo, "On the origin of satellite swarms," *Acta Astronaut.*, vol. 68, no. 7, pp. 1392–1395, Apr.–May 2011.
- [10] R. Radhakrishnan *et al.*, "Survey of inter-satellite communication for small satellite systems: Physical layer to network layer view," *IEEE Commun. Surveys Tuts.*, vol. 18, no. 4, pp. 2442–2473, 4th Quart. 2016.
- [11] G.-P. Liu and S. Zhang, "A survey on formation control of small satellites," *Proc. IEEE*, vol. 106, no. 3, Mar. 2018.
- [12] M. Röper, B. Matthiesen, D. Wübben, P. Popovski, and A. Dekorsy, "Beamspace MIMO for satellite swarms," in *Proc. IEEE Wireless Commun. Netw. Conf. (WCNC)*, Austin, TX, Apr. 2022.
- [13] —, "Distributed downlink precoding and equalization in satellite swarms," May 2022, submitted to *IEEE Trans. Wireless Commun.* [Online]. Available: <https://arxiv.org/abs/2205.11180>
- [14] J. Chu, X. Chen, C. Zhong, and Z. Zhang, "Robust design for noma-based multibeam leo satellite internet of things," *IEEE Internet Things J.*, vol. 8, no. 3, pp. 1959–1970, Feb. 2021.
- [15] W. Wang, L. Gao, R. Ding, J. Lei, L. You, C. A. Chan, and X. Gao, "Resource efficiency optimization for robust beamforming in multi-beam satellite communications," *IEEE Trans. Veh. Technol.*, vol. 70, no. 7, pp. 6958–6968, Jul. 2021.
- [16] Y. Liu, C. Li, J. Li, and L. Feng, "Robust energy-efficient hybrid beamforming design for massive mimo leo satellite communication systems," *IEEE Access*, vol. 10, pp. 63 085–63 099, Jun. 2022.
- [17] Z. Lin, M. Lin, Y. Huang, T. de Cola, and W.-P. Zhu, "Robust multi-objective beamforming for integrated satellite and high altitude platform network with imperfect channel state information," *IEEE Trans. Signal Process.*, vol. 67, no. 24, pp. 6384–6396, Dec. 2019.
- [18] S. Schwarz, "Robust full-dimension MIMO transmission based on limited feedback angular-domain CSIT," *J. Wireless Com. Network.*, no. 58, Mar. 2018.
- [19] M. Sadek, A. Tarighat, and A. H. Sayed, "Active antenna selection in multiuser MIMO communications," *IEEE Trans. Signal Process.*, vol. 55, no. 4, pp. 1498–1510, 2007.
- [20] L. You, K. X. Li, J. Wang, X. Gao, X. G. Xia, and B. Ottersten, "Massive MIMO transmission for LEO satellite communications," *IEEE J. Sel. Areas Commun.*, vol. 38, no. 8, pp. 1851–1865, Aug. 2020.
- [21] K. Storek, C. A. Hofmann, and A. Knopp, "Measurements of phase fluctuations for reliable MIMO space communications," in *Proc. IEEE Asia-Pac. Conf. Wireless Mob. (APWiMob)*, Bandung, Indonesia, Aug. 2015, pp. 157–162.
- [22] A. El Zooghby. Norwood, MA, USA: Artech House, 2005.
- [23] H. Kobayashi, B. L. Mark, and W. Turin, *Probability, Random Processes, and Statistical Analysis: Applications to Communications, Signal Processing, Queueing Theory and Mathematical Finance*. Cambridge University Press, 2011.
- [24] E. Telatar, "Capacity of multi-antenna gaussian channels," *Eur. Trans. Telecommun.*, vol. 10, no. 6, Nov.–Dec. 1999.
- [25] S. L. Ariyavisitakul, "Turbo space-time processing to improve wireless channel capacity," *IEEE Trans. Commun.*, no. 8, Aug. 2000.
- [26] R. W. Heath, Jr. and A. Lozano, *Foundations of MIMO Communication*. Cambridge, U.K.: Cambridge Univ. Press, 2019.
- [27] P. Patcharamaneepakorn, S. Armour, and A. Doufexi, "On the equivalence between SLNR and MMSE precoding schemes with single-antenna receivers," *IEEE Commun. Lett.*, vol. 16, no. 7, Jul. 2012.
- [28] F. Dietrich, *Robust Signal Processing for Wireless Communications*, ser. Foundations in Signal Processing, Communications and Networking. Springer-Verlag Berlin Heidelberg, 2008.
- [29] 3GPP, "Solutions for NR to support non-terrestrial networks (NTN)," *TR 38.821 V16.0.0*, Dec. 2019.
- [30] —, "Study on new radio (NR) to support non-terrestrial networks," *TR 38.811 V15.4.0*, Sep. 2020.
- [31] ITU-R, "Attenuation by atmospheric gases and related effects," *ITU-R P.676-12*, Aug. 2019.
- [32] —, "Propagation data and prediction method required for the design of Earth-space telecommunication systems," *ITU-R P.618-13*, Dec. 2017.
- [33] —, "Ionospheric propagation data and prediction methods required for the design of satellite networks and systems," *ITU-R P.531-14*, Aug. 2019.